PHILOSOPHICAL TRANSACTIONS OF THE ROYAL SOCIETY A MATHEMATICAL, PHYSICAL & ENGINEERING SCIENCES

Circuits and Simulations at 1 THz [and Discussion]

Christopher M. Snowden, D. Paul Steenson and D. Lippens

Phil. Trans. R. Soc. Lond. A 1996 **354**, 2435-2446
doi: 10.1098/rsta.1996.0110

Circuits and simulations at 1 THz

By Christopher M. Snowden and D. Paul Steenson

Microwave and Terahertz Technology Group, Department of Electronic and Electrical Engineering, University of Leeds, Leeds LS2 9JT, UK

The current state-of-the-art in device and circuit simulation, design and application for semiconductor devices operating in the terahertz regime is reviewed. The evolution of physical models to describe and investigate tunnelling and other ultra-small device structures is described. Simulations based on quantum hydrodynamic models and self-consistent solutions of the Poisson and Schrödinger equations, using analytical and numerical techniques are considered. Equivalent circuit extraction methods are considered, together with device models up to 2 THz. Examples of results obtained from simulations of terahertz devices are given, including resonant tunnelling structures. The design and modelling of circuits incorporating semiconductor tunnelling devices is discussed and illustrated with examples of recent developments. The challenges facing circuit designers and the potential applications for this technology are highlighted.

1. Introduction

The current major driving forces behind terahertz technology development remain the interest from space exploration authorities, remote sensing and future communications systems. A subtle change in the nature of the technology has been the shift in emphasis from detection of terahertz signals to the generation of power from local oscillators. This reflects the fact that the biggest challenge facing the terahertz community is the requirement for a solid-state RF source with useful output power and efficiency (typically greater than 100 μW and 1% for receiver applications), with acceptable noise performance. This will then allow the construction of compact low-power receivers and transmitters without the need for bulky external sources such as far-infrared lasers or travelling wave tubes. At present the advances in receiver design have already led to the development of 600 GHz quasi-optical SIS systems, and interest in developing non-cryogenically cooled systems is increasing rapidly.

The focus of this paper is to address the design and modelling of circuits and devices operating in the terahertz regime, with emphasis on tunnelling devices. One of the difficulties in developing a systematic method of designing both devices and circuits based on semiconductor tunnelling structures is the need to bridge the gap between theoretical principles and practical solutions. It is only relatively recently that physical models have begun to find a role in contemporary engineering design for more conventional devices (for example, microwave diodes and transistors). Physical models, based on hydrodynamic transport equations, have been shown to provide good agreement with experimental data for transferred electron devices and heterostructure barrier varactor diodes operating at frequencies up to 300 GHz (Curow

Phil. Trans. R. Soc. Lond. A (1996) **354**, 2435–2446
Printed in Great Britain

1995; Zybura *et al.* 1994, 1995). These simulations have provided a useful insight into both device and circuit design, linking the device model to the circuit model through a harmonic balance algorithm. At the present time, useful physical models are appearing which satisfactorily describe the operation of tunnelling structures suitable for terahertz applications. However, these models have still not found a place in circuit design because of their essentially qualitative results. In contrast, equivalent circuit models, which have long been the basis of design at lower frequencies, remain a key tool for submillimetre-wave circuit design. Results from the successful application of semiconductor tunnelling devices at terahertz frequencies are still very limited, although there has been considerable progress in demonstrating their operation at lower frequencies (for example, Steenson *et al.* 1994; Boric-Lubecke *et al.* 1995). Consequently, it is useful to consider the methods used for modelling and circuit design with 'conventional' devices, such as Schottky varactor diodes, operating at higher frequencies, as these may be applicable to tunnelling devices.

2. Diode simulation and circuits

(*a*) *Resonant tunnelling diodes*

The modelling of resonant tunnelling diodes (RTDs) is often considered in terms of either the static characteristics (including the I/V current–voltage characteristics) or the high-frequency properties. The majority of the effort to-date from a physical standpoint has been applied to the former, whilst the circuit designer desires a greater emphasis on the latter. The simulation of quantum semiconductor devices is usually based on one of four techniques: self-consistent quantum mechanical models (Liou & Roblin 1994), the density matrix method (Frensley 1985, 1988), Wigner function (Kluksdahl *et al.* 1989) or the quantum hydrodynamic method (Grubin & Kreskovsky 1989). The latter method has distinct advantages—it is computationally less intensive, the quantum hydrodynamic equations follow the form of the classical fluid dynamic quantities, and finally, well understood (classical) boundary conditions are used to simulate quantum devices. This approach has been successfully applied to the simulation of resonant tunnelling diodes with single and multiple regions of negative differential resistance (Gardner 1994, 1995). The quantum hydrodynamic model is based on the following equations for conservation of electron density, momentum and energy, respectively, coupled to the Poisson equation,

$$\frac{\partial n}{\partial t} + \frac{\partial}{\partial x_i}(nu_i) = 0, \tag{2.1}$$

$$\frac{\partial}{\partial t}(mnu_j) + \frac{\partial}{\partial x_i}(u_i mnu_j - P_{ij}) = -n\frac{\partial V}{\partial x_j} - \frac{mnu_j}{\tau_\mathrm{p}}, \tag{2.2}$$

$$\frac{\partial W}{\partial t} + \frac{\partial}{\partial x_i}(u_i W - u_j P_{ij} + q_i) = -nu_i\frac{\partial V}{\partial x_i} - \frac{(W - 2/3nT_0)}{\tau_\mathrm{w}}, \tag{2.3}$$

$$\nabla \cdot (\epsilon \nabla V) = q^2(n_\mathrm{D} - N_\mathrm{A} - n), \tag{2.4}$$

where n is the electron density, $\boldsymbol{u}$ is the velocity, m is the effective electron mass, i, j are spatial indices and the potential energy V is given by $V = -q\psi$ where ψ is the electrostatic potential. The stress tensor P_{ij} and energy density W incorporate quantum mechanical effects, which following the work of Ancona & co-workers (1987,

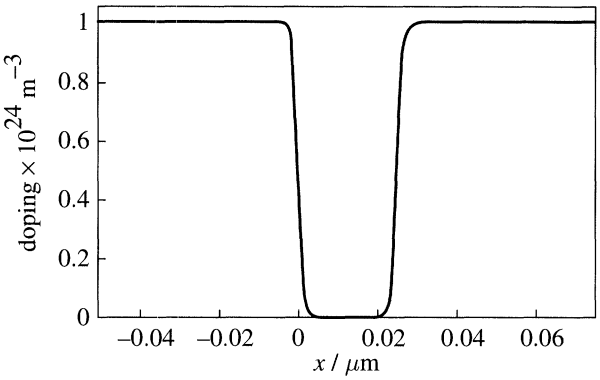

Figure 1. Doping profile of a double-barrier GaAs–AlGaAs resonant tunnelling diode (Chen *et al.* 1995).

1989) and Gardner (1994), and assuming the $O(\hbar^2)$ momentum-shifted thermal equilibrium Wigner distribution function (Wigner 1932) yields

$$P_{ij} = -nT\delta_{ij} + \frac{\hbar n}{12m}\frac{\partial^2}{\partial x_i \partial x_j}\log(n) + O(\hbar^4), \tag{2.5}$$

$$W = \frac{3}{2}nT + \frac{1}{2}mnu^2 - \frac{\hbar^2 n}{24m}\nabla^2 \log(n) + O(\hbar^4). \tag{2.6}$$

It should be noted that this model retains the relaxation time approximation in the classical collision terms of equations (2.2) and (2.3) and that the heat flux follows the relation $\boldsymbol{q} = -\kappa\nabla T$ (Fourier's law), where T is the electron temperature.

In one dimension the quantum hydrodynamic model has two Schrödinger modes (a parabolic and an elliptic mode), requiring eight boundary conditions. In the case of the resonant tunnelling diode Gardner suggests the following boundary conditions:

$$n = N_{\mathrm{D}} \quad \frac{\partial n}{\partial x} = 0 \quad \frac{\partial T}{\partial x} = 0 \quad \text{at boundaries } x_{\mathrm{L}} \text{ and } x_{\mathrm{R}}, \tag{2.7}$$

$$V(x_{\mathrm{L}}) = T\log\left(\frac{n}{n_i}\right), \quad V(x_{\mathrm{R}}) = T\log\left(\frac{n}{n_i}\right) + \Delta V, \tag{2.8}$$

where n_{i} is the intrinsic electron concentration and ΔV is the bias voltage across the device.

Chen *et al.* (1995) have used the quantum hydrodynamic model to investigate the operation of GaAs resonant-tunnelling diodes with double barriers (figure 1). Typical conduction band energy, electron density results obtained from this simulation are shown in figure 2. The I–V characteristics of the resonant-tunnelling diode are shown in figure 3. Hysteresis was observed in the simulated results and this is depicted in figures 1–3 by arrows and the use of dark and lighter lines.

Liou & Roblin (1994) have described a high-frequency simulation of resonant tunnelling diodes based on a self-consistent Poisson–Schrödinger solution. The Poisson and Schrödinger equations are solved self-consistently for each harmonic using a harmonic-balance technique. They confirmed that the RTD exhibits an increased capacitance in the negative differential conductance region in agreement with experimental data. They also concluded that the derivation of the RTD capacitance from a quasi-static analysis using the differential variation of the DC charge in the RTD is not

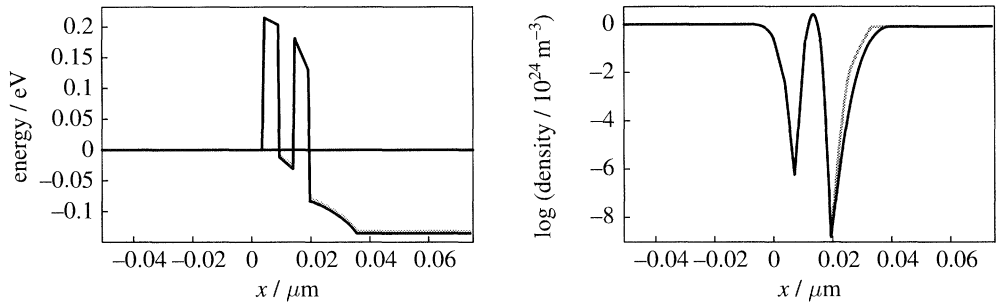

Figure 2. (*a*) Conduction band energy and (*b*) electron density for $\Delta V = 0.135$ V (Chen *et al.* 1995).

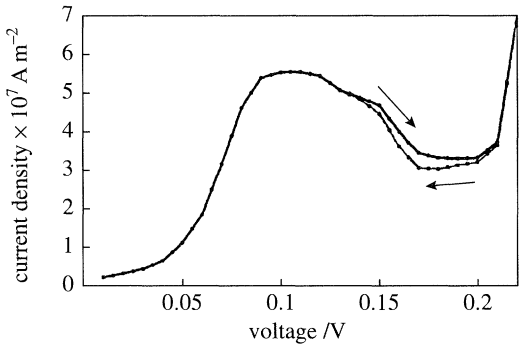

Figure 3. *I*–*V* characteristics of the RTD in figure 1 (Chen *et al.* 1995).

applicable because the RTD well charges through the cathode, but discharges through the anode. They also obtained a variation in conductance and susceptance similar to that observed in experimental data. A large frequency dependence of the admittance is only observed when the RTD is biased in the negative differential conductance region and a reduction in the RTD conductance and capacitance is observed. These observations illustrate the need for fully self-consistent time-dependent analyses in relation to devices reliant on quantum transport effects. The frequency dependence is modelled in an equivalent circuit by using a quantum inductance in series with the negative resistance of the RTD, figure 4.

The work of Liou & Roblin (1994) indicates that for the RTD structures they considered, a useful negative conductance ($G \leftarrow 0.02$ S) is observable to beyond 1.6 THz. They also observed a decrease in $|G|$ with increasing frequency occurring at as little as 150 GHz. However, this phenomenological decrease in $|G|$ was accompanied by a simultaneous reduction in capacitance C with frequency. The combined effect was a weaker frequency dependence than would otherwise have been expected. Another, significant finding from their analysis is that, under large signal ($qV_{\mathrm{ac}} \gg h\omega/2\pi$) conditions, $|G|$ decreases with increasing signal amplitude, in a similar fashion to trends observed in other two-terminal negative resistance devices (TEDs, IMPATT diodes), which is consistent with basic one-port oscillator theory. These effects have an obvious relevance to the high-frequency application of such devices. The frequency limit for oscillation in the simulation of Liou & Roblin (1994) was dictated by the series resistance R_{S}, and the frequency dependence of the negative conductance. Smith *et al.* (1994) have addressed the issue of R_{S} experimentally and have developed techniques to extend the working frequency range of GaAs–AlAs RTD's to 900 GHz using

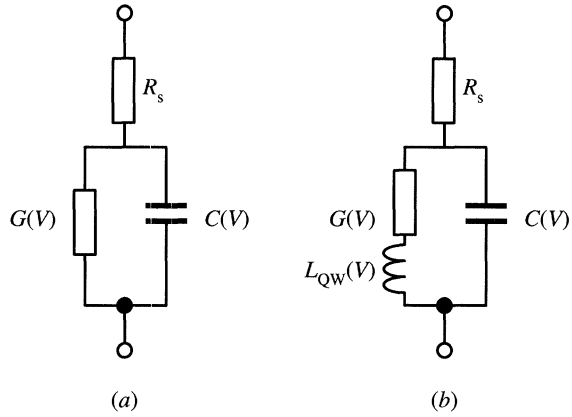

Figure 4. Equivalent circuit models of resonant tunnelling diodes: (*a*) low-frequency model; (*b*) large-signal model with frequency-independent elements (after Brown *et al.* 1989).

a Schottky collector contact. The use of Schottky collector contacts also favours improved heat-sinking and simplifies the processing considerably but may increase the noise figure of such devices if used as detectors rather than oscillators.

The rigorous design of terahertz circuits incorporating tunnelling devices is perhaps less well explored than their physics and modelling, despite the clear potential of these devices being known for several years (see, for example, Brown *et al.* 1991; Smith *et al.* 1994). In the case of RTDs, a fundamental difficulty faced by circuit designers is the relatively low output powers obtainable. This has led to considerable effort in examining methods of achieving efficient power combining. Boric-Lubecke *et al.* (1995) have shown that connecting several RTDs in series is a feasible method for increasing power output when these devices are configured as oscillators, although results have been limited to a proof-of-concept experiment at 2 GHz.

Steenson *et al.* (1994) have demonstrated coherent power combining of two RTD devices in the W-band, using a Kurokawa (1978) type approach, and have investigated the possibility of hierarchical combining which could be extended to encompass, layer level (such as the Boric–Lubecke, series connection), chip level (lumped circuit) and circuit level (distributed) combining. An alternative method of obtaining higher output powers may be to utilize planar arrays of diodes and transistors in a single waveguide cavity (Adams *et al.* 1995). This has also been shown to work for Gunn diodes, configured to act as a frequency doubler, generating power at 170 GHz (Tuovinen & Erickson 1995). Unfortunately, at frequencies much above 100 GHz metallic waveguide dimensions become restrictive; for example, at 200 GHz the waveguide dimensions are $1.3 \times 0.65\ \mathrm{mm}^2$. These limitations favour novel approaches, such as dielectric waveguides, quasi-optics (Kim *et al.* 1993), integrated on-chip low-loss rectangular waveguides (Treen & Cronin 1993; Brown *et al.* 1994) or more probably, combinations of technologies which exploit the strengths of each.

(*b*) *Schottky diodes and heterostructure barrier varactor diodes*

Schottky diodes form a key element in submillimetre-wave receivers configured as detectors or multipliers (varactor diodes). In these very small devices the diameter of the diode is relatively small and comparable to the device thickness (figure 6). This leads to a non-uniform potential distribution and curved depletion layer boundaries (reverse bias) as the edge effects and surface depletion (in compound semiconductor

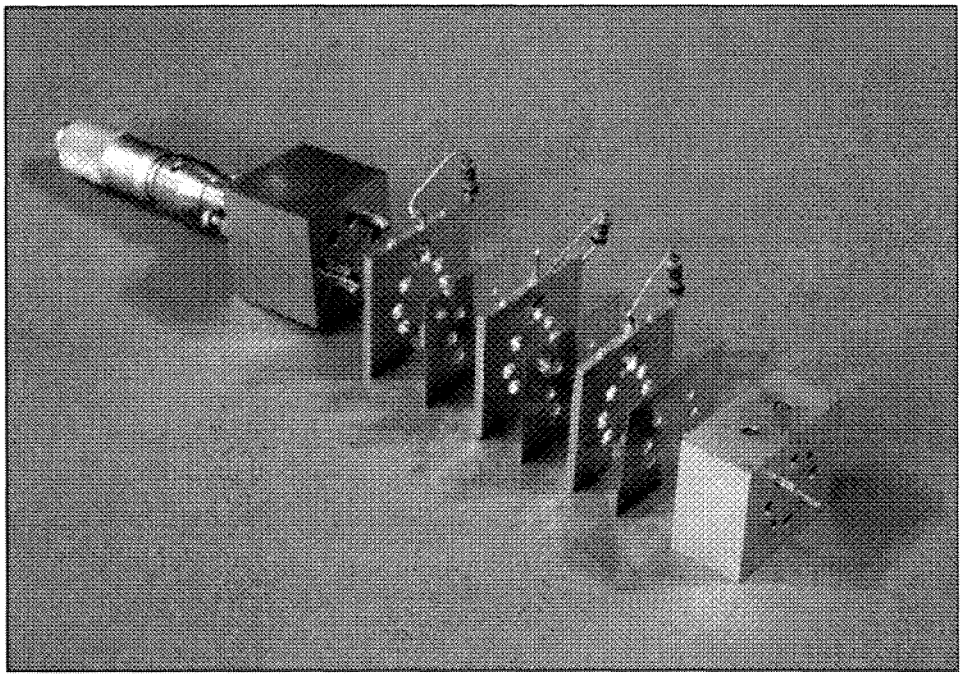

Figure 5. W-bond waveguide circuit for power combining three resonant tunelling diodes (Steenson *et al.* 1994).

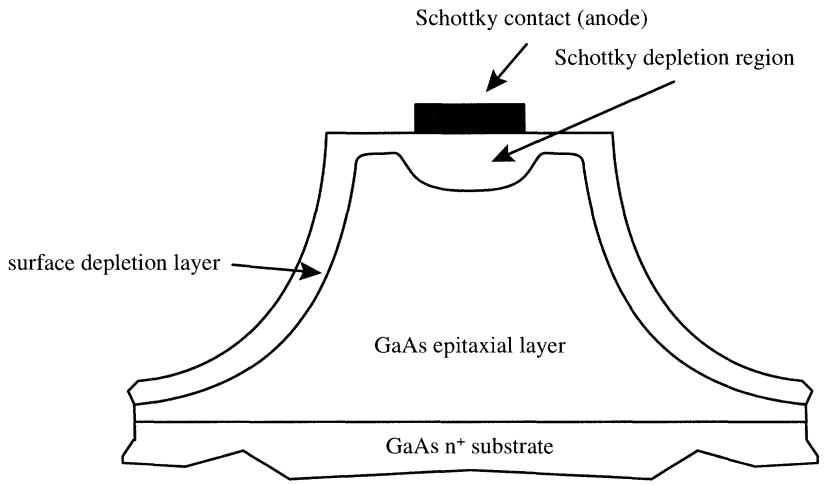

Figure 6. Cross-section of submillimetre-wave Schottky diode (reverse bias).

devices) substantially modify the characteristics of the diode, which are especially significant with shrinking dimensions.

The majority of engineering models used in circuit designs are based on equivalent circuit models. At terahertz frequencies these models must account for carrier inertia and dielectric displacement current effects, in addition to edge effects (Crowe 1989). Louhi & Räisänen (1995) have developed a Schottky varactor diode model, shown in figure 7, which accounts for edge effects and non-uniform charge distributions associated with the junction capacitance and series resistance. Furthermore, they have

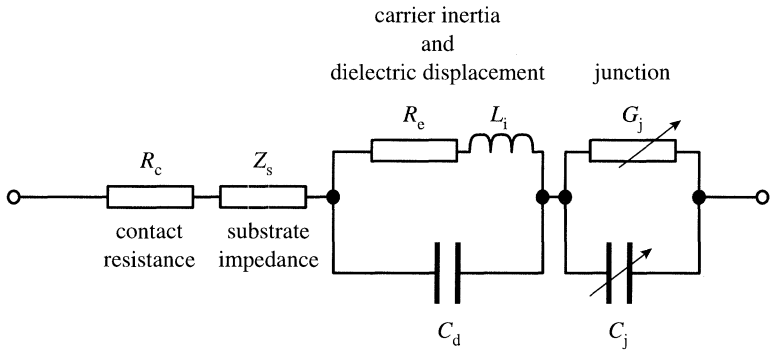

Figure 7. Terahertz Schottky varactor diode equivalent circuit model (after Louhi & Raisanen 1995).

investigated the role of velocity saturation (first considered by Kollberg *et al.* 1992) in determining the maximum output power of the Schottky varactor frequency multipliers at submillimetre wavelengths. They conclude that edge effects and velocity saturation significantly affect the modelling of these diodes and verified their model for a balanced doubler operating at 160 GHz. They also predicted that the maximum theoretical output power of a Schottky varactor diode triplet operating at 1 THz is in the region of 250 μW.

East (1995) has considered the impact of current saturation effects on limiting the high-frequency performance of Schottky barrier mixers and multipliers. The significance of this effect was observed four years previously and reported at the Second International Conference on Space Terahertz Technology (Pasadena, CA). East has applied a large-signal time-dependent Monte Carlo simulation to the modelling of Schottky barrier mixers and varactor diodes. The results of this study reveal that GaAs varactor diodes operating above 100 GHz are limited by valley transfer effects, resulting in an accumulation of hot electrons in the neutral region of the device in the high-voltage portion of the RF cycle. These electrons do not have sufficient time to thermalize in the remaining part of the cycle, which leads to an increases in the resistance and a reduction in RF performance. Furthermore, in the case of mixers, operating in forward bias, an inductive current delay causes an under-damped resonant current flow at the device terminals. An inductive delay occurs in a material when the electron motion cannot follow a rapidly changing field. In the case of GaAs this effect becomes significant above 500 GHz.

The role of tunnelling in the operation of heterostructure barrier varactor diodes (HBVs) has been considered recently by Jones *et al.* (1995). This work is based on a hydrodynamic simulation which incorporates bulk transport, transport across heterointerfaces (thermionic and thermionic-field emission) and barrier tunnelling. HBV simulations were performed at 100 GHz and demonstrated the feasibility of extracting power at the third harmonic.

(*c*) *Circuits*

The design and modelling of circuits above 200 GHz is still relatively uncommon, other than for applications in radio astronomy. The typical modelling approaches are extensions of existing analytical techniques for strip transmission line systems, with complementary information supplied from scale models, usually at an order of magnitude lower in frequency. Recently, finite-difference time-domain (FDTD) electro-

magnetic analysis techniques (Siegel *et al.* 1991; Oswald *et al.* 1994) have been used to determine the embedding impedance of waveguide mount structures at terahertz frequencies, and have shown a marked improvement on the previous solutions based on simplified solutions of dyadic Green's functions (Eisenhart & Khan 1971). The FDTD technique is also applicable to strip transmission lines, and in the future should allow system level designs to be analysed and extended to nonlinear components. Promising transmission line environments for terahertz circuits are: planar circuits on low dielectric constant–low-loss membranes, metal-pipe on-wafer waveguides, image-guide and quasi-optics. The propagation velocities in some typical planar guided-wave structures at 200 GHz are shown here for comparison, normalized to the speed of light: 0.375 for coplanar waveguide (CPW) on GaAs, 0.9 for a SiO_2 membrane (Cheng *et al.* 1994), 0.73 for elevated CPW on polyimide (Bhattacharya *et al.* 1995). Mathematical techniques already exist for modelling 'conventional' guided-wave environments, but further development is required to make available more general electromagnetic analytical techniques, such as spectral domain, finite-element, finite-difference time-domain, transmission line matrix (AlBasha *et al.* 1995) methods, which can be used for sensitivity and optimization analysis of general, but complex, three-dimensional problems. Similarly, techniques for modelling quasi-optic circuits are relatively well established (Martin & Bowen 1993; York 1993). From the point of view of true terahertz device and circuit embedding techniques, it would be desirable to use integrated lumped element tuning circuits where 'active' devices could be used as shunt tuning capacitors, and electrically short lengths of line, as inductors (Zmuidzinas *et al.* 1994), it may also prove possible to exploit carrier inertia effects as series or shunt tuning inductances.

3. Transistor circuits for terahertz applications

One of the issues surrounding solid-state terahertz technology is the question of whether transistor circuits will ever be able to offer useful levels of power at these frequencies. Until recently, it was widely held that transistors would be unable to satisfy system requirements above 100 GHz. InP HEMT technology has begun to show promise for applications above this frequency, with cut-off frequencies higher than 300 GHz being obtained for 0.1 μm gate length FETs (Wojtowicz *et al.* 1994). It has already been successfully demonstrated that 50 nm gate length AlInAs–GaInAs–InP HEMTs can provided useful power at 13 GHz when configured as an oscillator in a quasi-optical circuit (Rosenbaum *et al.* 1995).

There is considerable emphasis currently being placed on developing transistors for operation at frequencies above 100 GHz. The extension of heterojunction bipolar transistors into the millimetre and submillimetre wave regimes includes work on hot electron transistors, which reduce transit times by injecting hot electrons into the base region, which traverse this region ballistically (Ingram *et al.* 1995). Double-heterojunction InP–InGaAs bipolar transistors with DC current gains in excess of 200, have demonstrated current gain cut-off frequencies of up to 155 GHz (Kurishima *et al.* 1994), utilizing compositionally step-graded InGaAsP layers between the InGaAs base and InP collector to suppress current blocking effects. A key aspect of this development was the demonstration of the significant role of non-equilibrium transport in determining the high-frequency performance.

Recently, resonant tunnelling bipolar transistors (RTBTs) have begun to demonstrate potential for microwave applications, with unity gain cut-off frequencies of

above 20 GHz (Koch *et al.* 1994), but have not shown the necessary cut-off frequencies appropriate for terahertz circuits. In the InGaAs transistor of Koch *et al.*, the base behaves as a coupled quantum well, with a base transit time of approximately 4 ps (the principal limiting factor in this design). Similar high-frequency performance has been reported by Moise *et al.* (1994) who have developed an integrated amplifiers with resonant-tunnelling transistors and tunnelling hot-electron transistors. These circuits were found to have current gain cut-off frequencies in the region of 20 GHz. Seabaugh *et al.* (1993) have reported integrated circuits incorporating resonant tunnelling and double-heterojunction transistors on the same die, with an $f_{\max}$ of 21 GHz. These circuits and those of Moise *et al.* (1993), both from Texas Instruments, were aimed at high-speed logic circuit applications, where the NDR aspect of the devices is suited to multi-state logic together with the advantage of reduced component count. Novel applications are also possible using the InGaAs coupled-quantum-well base transistor (Koch *et al.* 1994), such as a phototransistor with apparent photo-bistability. The maximum operating frequency of such devices needs to be extended and will require accurate device models to help accomplish this.

The modelling of RTBTs has addressed both self-consistent calculation of the tunnelling current (see, for example, Bigelow *et al.* (1994), who self-consistently solve the Poisson and Schrödinger equations with a transfer-Hamiltonian formalism), and distributed effects (Taniyama *et al.* (1994), who developed a two-dimensional quantum distributed model). Two-dimensional simulations have shown spatial variations in the current density and that the resonance of the collector current is reduced when the spatial variation of the well potential is large.

4. Conclusions and the future

The simulation and design of semiconductor tunnelling devices and their application in circuits intended for operation at terahertz frequencies is still at an early stage. Quantum device models are providing useful tools for both device and device-circuit interaction studies. Such models must cater for pseudomorphic material interfaces, and increasingly complex time-dependent carrier transport phenomena. The majority of engineering solutions are still based on equivalent circuit models, suitably adapted to reflect the device behaviour at terahertz frequencies. The increasing utilization of three-dimensional electromagnetic field solvers provides the terahertz circuit designer with a powerful tool to investigate passive structures, which ideally requires interfacing to suitable active device simulators.

The utilization of semiconductor tunnelling devices at terahertz frequencies will depend on their ability to meet the system performance requirements together with the availability of accurate modelling and design techniques, coupled to suitable circuit technologies. At the present time simulation and modelling techniques are providing greater insight into the operation of these devices and have the potential to provide circuit designers with a useful basis for developing subsystems.

The authors acknowledge contributions from J. Jerome of Northwest University, C. Gardner of Duke University, J. East and G. Rebeiz from the University of Michigan.

References

Adams, A., Pollard, R. D. & Snowden, C. M. 1995 Multiple oscillator resonant power combining. In *Proc. European Microwaves Conf.* (Bologne), pp. 1068–1073.

PHILOSOPHICAL TRANSACTIONS OF THE ROYAL SOCIETY A MATHEMATICAL, PHYSICAL & ENGINEERING SCIENCES

Albasha, L. & Snowden, C. M. 1994 An integrated simulation technique for the modelling of lumped elements using the TLM method. *Proc. 24th European Microwave Conf.*, vol. 1, pp. 848–853.

Ancona, M. G. & Tiersten, H. F. 1987 Macroscopic physics of the silicon inversion layer. *Phys. Rev.* B **35**, 7959–7965.

Ancona, M. G. & Iafrate, G. J. 1989 Quantum correction to the equation of state of an electron gas in a semiconductor. *Phys. Rev.* B **39**, 9536–9540.

Bigelow, J. M. & Leburton, J. P. 1994 Self-consistent modeling of resonant interband tunnelling in bipolar tunnelling field-effect transistors. *IEEE Trans. Electron Dev.* **41**, 125–131.

Bhattacharya, U., Allen, S. T. & Rodwell, M. J. W. 1995 DC–725 GHz sampling circuits and subpicosecond nonlinear transmission lines using elevated coplanar waveguide. *IEEE Microwave Guided Wave Lett.* **5**, 50–52.

Boric-Lubecke, O., Pan, D.-S. & Itoh, T. 1995 Fundamental and subharmonic excitation for an oscillator with several tunnelling diodes in series. *IEEE Trans. Microwave Theory Techn.* **43**, 969–976.

Brown, D. A., Treen, A. S. & Cronin, N. J. 1994 Micromachining of terahertz waveguide components with integrated active devices. In *19th Int. Conf. on Infrared and Millimetre Waves* (Sendai).

Brown, E. R., Parker, C. D. & Sollner, T. C. L. G. 1989 Effect of quasibound-state lifetime on the oscillation power of resonant tunnelling diodes. *Appl. Phys. Lett.* **54**, 934–936.

Brown, E. R., Söderström, J. R., Parker, C. D., Mahoney, L. J., Molvar, K. M. & McGill, T. C. 1991 Oscillations up to 712 GHz in InAs/AlSb resonant-tunnelling diodes. *Appl. Phys. Lett.* **58**, 2291.

Chen, Z., Cockburn, B., Gardner, C. & Jerome, J. W. 1995 Quantum hydrodynamic simulation of hysteresis in the resonant tunneling diode. *J. Comput. Phys.* **117**, 274–280.

Cheng, H., Whitaker, J. F., Weller, T. M. & Katehi, L. P. B. 1994 Terahertz-bandwidth pulse propagation on a coplanar stripline fabricated on a thin membrane. *IEEE Microwave Guided Wave Lett.* **4**, 89–91.

Crowe, T. W. 1989 GaAs Schottky barrier mixer diodes for the frequency range 1–10 THz. *Int. J. Infrared Millimetre Waves* **10**, 765–777.

Curow, M. 1995 New insight in operation principles and accurate design of fundamental and harmonic millimeter-wave oscillators. *IEEE Proc. MTT-S Conf.*, pp. 545–548.

East, J. 1995 Monte Carlo simulation of Schottky barrier mixers and varactors. *6th Int. Conf. on Space Terahertz Technology.*

Eisenhart, R. L. & Khan, P. J. 1971 Theoretical and experimental analysis of a waveguide mounting structure. *IEEE Trans. Microwave Theory Techn.* **19**, 706–719.

Frensley, W. R. 1985 Simulation of resonant-tunnelling heterostructure devices. *J. Vac. Sci. Technol.* B **3**, 1261–1266.

Frensley, W. R. 1988 Quantum transport calculation of the frequency response of resonant-tunnelling heterostructure devices. *Superlattices Microstructures* **4**, 497–501.

Gardner, C. L. 1994 The quantum hydrodynamic model for semiconductor devices. *SIAM J. Appl. Math.* **54**, 409–427.

Gardner, C. L. 1995 Resonant tunnelling in the quantum hydrodynamic model. *VLSI Design* (In the press.)

Grubin, H. L. & Kreskovsky, J. P. 1989 Quantum moment balance equations and resonant tunnelling structures. *Solid-State Electron.* **32**, 1071–1075.

Ingram, S. G., Linfield, E. H., Brown, K. M., Jones, G. A. C., Ritchie, D. A. & Kelly, M. J. 1995 2DEG base hot electron transistors fabricated using MBE and in sitution beam lithography. *IEEE Trans. Electron Dev.* **42**, 1065–1069.

Jones, J. R., Tait, G. B., Jones, S. H. & Katzer, D. S. 1995 DC and large-signal time-dependent electron transport in heterostructure devices: an investigation of the heterostructure barrier varactor. *IEEE Trans. Electron Dev.* **42**, 1070–1080.

Kim, M., Sovero, E., Hacker, J., De Lisio, M., Chiao, J., Li, S., Gagnon, D., Rosenberg, J. & Rutledge, D. 1993 A 100 element HBT grid amplifier. *IEEE Trans. Microwave Theory Techn.* **41**, 1762–1771.

PHILOSOPHICAL TRANSACTIONS OF THE ROYAL SOCIETY A MATHEMATICAL, PHYSICAL & ENGINEERING SCIENCES

Kluksdahl, N. C., Kriman, A. M., Ferry, D. K. & Ringhofer, C. 1989 Self-consistent study of the resonant-tunnelling diode. *Phys. Rev.* B **39**, 7720–7735.

Koch, S., Waho, T. & Mizutani, T. 1994 InGaAs resonant tunnelling transistors using a coupled-quantum-well base with strained AlAs tunnel barriers. *IEEE Trans. Electron Dev.* **41**, 1498–1503.

Kollberg, E. L., Tolmunen, T. J., Frerking, M. A. & East, J. A. 1992 Current saturation in submillimetre wave varactors. *IEEE Trans. Microwave Theory Techn.* **40**, 831–838.

Kurishima, K., Nakajima, H., Kobayashi, T., Matsuoka, Y. & Ishibashi, T. 1994 Fabrication and characterisation of high performance InP/InGaAs double-heterojunction bipolar transistors. *IEEE Trans. Electron Dev.* **41**, 1319–1326.

Kurokawa, K. 1978 Microwave solid-state oscillator circuits. *Microwave devices, device circuit interactions* (ed. M. J. Howes & D. V. Morgan), pp. 207–265. New York: Wiley.

Liou, W.-R. & Roblin, P. 1994 High frequency simulation of resonant tunnelling diodes. *IEEE Trans. Electron Dev.* **41**, 1098–1111

Louhi, J. T. & Räisänen, A. V. 1995 On the modeling and optimization of Schottky varactor frequency multipliers at submillimetre wavelengths. *IEEE Trans. Microwave Theory Techn.* **43**, 922–926.

Martin, D. H. & Bowen, J. W. 1993 Long-wave optics. *IEEE Microwave Theory Techn.* **41**, 1676–1691.

Moise, T. S., Seabaugh, A. C., Beam, E. A. & Randall, J. N. 1993 Room-temperature operation of resonant-tunneling hot-electron transistor based integrated circuit. *IEEE Electron Dev. Lett.* **14**, 441–443.

Moise, T. S., Kao, Y.-C., Seabaugh, A. C. & Taddiken, A. H. 1994 Integration of resonant tunneling transitors and hot-electron transitors. *IEEE Electron Dev. Lett.* **15**, 254–256.

Oswald, J. E., Siegel, P. H. & Ali, S. M. 1994 Finite difference time domain analysis of coplanar transmission line circuits and a post-gap waveguide mounting structure. *5th Int. Symp. on Space Terahertz Technology* (Michigan), pp. 700–719.

Rosenbaum, S. E., Kormanyos, B. K., Jelloian, L. M., Matloubian, M., Brown, A.A, Larson, L. E., Nguyen, L. D., Thompson, M. A., Katehi, L. P. B. & Rebeiz, G. M. 1995 155- and 213 GHz AlInAs/GaInAs/InP HEMT MMIC oscillators. *IEEE Trans. Microwave Theory Techn.* **43**, 927–932.

Seabaugh, A. C., Beam III, E. A., Taddiken, A. H., Randall, J. N. & Kao, Y.-C. 1993 *IEEE Electron Dev. Lett.* **14**, 472–474.

Siegel, P. H., Oswald, J. E., Dengler, R. J., Sheen, D. M. & Ali, S. M. 1991 Measured and computed performance of a microstrip filter composed of semi-insulating GaAs on fused quartz substrate. *IEEE Microwave Guided Wave Lett.* **1**, 78–80.

Smith, R. P., Allen, S. T., Reddy, M., Martin, S. C., Liu, J., Muller, R. E. & Rodwell, M. J. W. 1994 0.1 μm Schottky-collector AlAs/GaAs resonant tunneling diodes. *IEEE Electron Dev. Lett.* **15**, 295–297.

Steenson, D. P., Miles, R. E., Pollard, R. D., Chamberlian, J. M. & Henini, M. 1994 Demonstration of power combining at W-band from GaAs/AlAs resonant tunnelling diodes. *5th Int. Symp. on Space Terahertz Technology*, pp. 756–767.

Taniyama, H., Tomizawa, M. & Yoshii, A. 1994 Quantum distributed model of the resonant tunneling transistor. *IEEE Trans. Electron Dev.* **41**, 294–297.

Treen, A. S. & Cronin, N. J. 1993 Terahertz metal pipe waveguides. *18th Int. Conf. on Infrared and Millimetre waves* (Essex).

Tuovinen, J. & Erickson, N. R. 1995 Analysis of a 170 GHz frequency doubler with an array of planar diodes. *IEEE Trans. Microwave Theory Techn.* **43**, 962–968.

Wigner, E. 1932 On the quantum correction for thermodynamic equilibrium. *Phys. Rev.* **40**, 749–759.

Wojtowicz, M., Lai, R., Streit, D. C., Ng, G. I., Block, T. R., Tan, K. L., Liu, P. H., Freudenthal, A. K. & Dia, R. M. 1994 0.10 μm graded InGaAs channel InP HEMT with 305 GHz f_T and 340 GHz f_{max}. *IEEE Electron Dev. Lett.* **15**, 477–479.

York, R. A. 1993 Nonlinear analysis of phase relationships in quasi-optical oscillator arrays. *MTT* **41**, 1799–1809.

PHILOSOPHICAL TRANSACTIONS OF THE ROYAL SOCIETY A MATHEMATICAL, PHYSICAL & ENGINEERING SCIENCES

Zmuidzinas, J., LeDuc, H. D., Stern, J. A. & Cypher, S. R. 1994 Two-junction tuning circuits for submillimetre SIS mixers. *MTT* **42**, 698–706.

Zybura, M. F., Tait, G. B, Jones, S. H. & Jones, J. R. 1994 100–300 GHz Gunn oscillator simulation through harmonic balance circuit analysis linked to a hydrodynamic device simulator. *IEEE Microwave Guided Lett.* **4**, 282–284.

Zybura, M. F., Jones, J. R, Jones, S. H. & Tait, G. B. 1995 Simulation of 100–300 GHz solid-state harmonic sources. *IEEE Trans. Microwave Theory Techn.* **43**, 955–961.

Discussion

D. LIPPENS (*Institut d'Electronique et de Microélectronique du Nord, Université des Sciences et Technologies de Villeneuve d'Ascq, France*). The intrinsic high-frequency characteristics of resonant tunnelling diodes (RTDs) are still an open issue. The key question is whether the reactive feature of RTDs is inductive or capacitive. Early on, it was recognized that the current flowing through such a quantum structure cannot basically follow a very fast voltage modulation due to the finite lifetime (τ) of the carriers in the quantum well. Until now, several equivalent circuits have been proposed to account for these effects, notably with the addition of an intrinsic self-inductance in series with the negative differential resistance (NDR) (Brown *et al.* 1989). The main problem concerning this kind of lumped circuit is that the intrinsic inductance L_w (equal to $R\tau$) is negative in the NDR bias region and under these conditions the physical meaning is not straightforward. Experimentally however, it was demonstrated that such an equivalent circuit is able to provide an accurate description of the frequency evolution of impedance of thick-barrier RTDs and hence with long carrier lifetimes in the well. Also, it can be shown that other circuit schemes, notably in the configuration of two RC subcircuits in series, according to the sequential picture of the resonant tunnelling effect, can also reproduce the impedance data versus frequency (Vanbésian *et al.* 1992). In this context an ambiguity still exists. Also, theoretically the subject remains controversial as shown in Fernando & Frensley (1995), who have found a complex frequency and bias dependence of the reactive current component.

Additional references

Brown, E. R., Parker, C. D. & Sollner, T. C. L. G. 1989 *Appl. Phys. Lett.* **54**, 934.

Vanbésien, O., Sadaune, V., Lippens, D., Vinter, B., Bois, P. & Nagle, J. 1992 *Microwave Opt. Technol. Lett.* **5**, 351.

Fernando, C. L. & Frensley, W. R. 1995 *Phys. Rev.* B **52**, 5092.

PHILOSOPHICAL TRANSACTIONS OF THE ROYAL SOCIETY A MATHEMATICAL, PHYSICAL & ENGINEERING SCIENCES

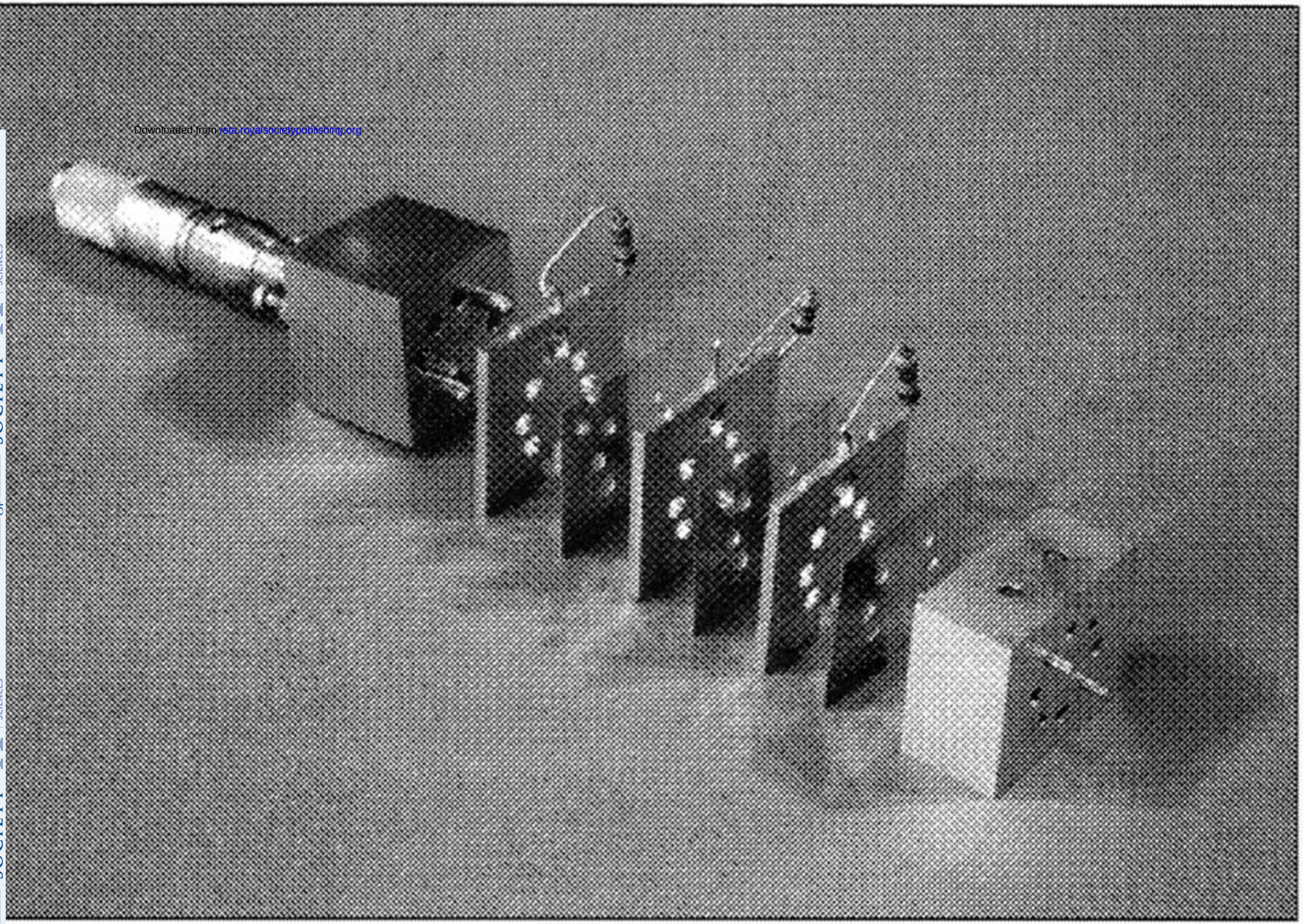

igure 5. W-bond waveguide circuit for power combining three resonant tunelling diodes (Steenson *et al.* 1994).